

1 Title

2

3 **Eddy Covariance Evaluation of Ecosystem Fluxes at a Temperate Saltmarsh in**  
4 **Victoria, Australia Shows Large CO<sub>2</sub> Uptake**

5

6 Authors

7

8 Ruth Reef<sup>1</sup>,

9 Edoardo Daly<sup>2,3</sup>,

10 Tivanka Anandappa<sup>1</sup>,

11 Eboni-Jane Vienna-Hallam<sup>1</sup>,

12 Harriet Robertson<sup>1</sup>,

13 Matthew Peck<sup>1</sup>,

14 Adrien Guyot<sup>4,5</sup>

15

16 Affiliations

17

18 1 School of Earth, Atmosphere and Environment, Monash University, VIC 3800, Australia

19 2 Department of Civil Engineering, Monash University, VIC 3800, Australia

20 3 WMAwater, Brisbane, QLD 4000, Australia

21 4 Atmospheric Observations Research Group, The University of Queensland, Brisbane,  
22 Australia

23 5 Australian Bureau of Meteorology, Melbourne, Australia

24

25 Corresponding Author

26

27 Associate Professor Ruth Reef

28 School of Earth Atmosphere and Environment

29 Monash University

30 9 Rainforest Walk, Clayton VIC 3800

31 Australia

32 Email: [ruth.reef@monash.edu](mailto:ruth.reef@monash.edu)

33 Ph: +61 3 9905 8309

34

35

36 Key Points

37

38 This is the first study using eddy covariance to measure CO<sub>2</sub> fluxes at an Australian  
39 temperate saltmarsh, revealing temperature and light limitations to CO<sub>2</sub> uptake.

40

41 CO<sub>2</sub> fluxes varied seasonally; growing season net ecosystem productivity was 10.54 g CO<sub>2</sub>  
42 m<sup>-2</sup> day<sup>-1</sup>, dropping to 1.64 g CO<sub>2</sub> m<sup>-2</sup> day<sup>-1</sup> in winter.

43

44 Productivity at the French Island saltmarsh is high relative to global saltmarsh estimates but  
45 below global mangrove averages.

46

47

48

49 Abstract

50

51 Recent studies highlight the important role of vegetated coastal ecosystems in atmospheric  
52 carbon sequestration. Saltmarshes constitute 30% of these ecosystems globally and are the  
53 primary intertidal coastal wetland habitat outside the tropics. Eddy covariance (EC) is the  
54 main method for measuring biosphere-atmosphere fluxes, but its use in coastal environments  
55 is rare. At an Australian temperate saltmarsh site on French Island, Victoria, we measured  
56 CO<sub>2</sub> and water gas concentration gradients, temperature, wind speed and radiation. The  
57 marsh was dominated by a dense cover of *Sarcocornia quinqueflora*. Fluxes were seasonal,  
58 with minima in winter when vegetation is dormant. Net ecosystem productivity (NEP) during  
59 the growing season averaged 10.54 g CO<sub>2</sub> m<sup>-2</sup> day<sup>-1</sup> decreasing to 1.64 g CO<sub>2</sub> m<sup>-2</sup> day<sup>-1</sup> in  
60 the dormant period, yet the marsh remained a CO<sub>2</sub> sink due to some sempervirent species.

61 Ecosystem respiration rates were lower during the dormant period compared with the  
62 growing season (1.00 vs 1.77 μmol CO<sub>2</sub> m<sup>-2</sup> s<sup>-1</sup>) with a slight positive relationship with  
63 temperature. During the growing season, fluxes were significantly influenced by light levels,  
64 ambient temperatures and humidity with cool temperatures and cloud cover limiting NEP.

65 Ecosystem water use efficiency of 0.86 g C kg<sup>-1</sup> H<sub>2</sub>O was similar to other C<sub>3</sub> intertidal  
66 marshes and evapotranspiration averaged 2.48 mm day<sup>-1</sup> during the growing season.

67

68 EGUsphere Topics

69 Emissions, Marine and Freshwater Biogeosciences, Earth System Biogeosciences

70

71 Short Summary

72

73 Studies show that saltmarshes excel at capturing carbon from the atmosphere. In this study,  
74 we measured CO<sub>2</sub> flux in an Australian temperate saltmarsh on French Island. The temperate  
75 saltmarsh exhibited strong seasonality. During the warmer growing season, the saltmarsh  
76 absorbed on average 10.5 grams of CO<sub>2</sub> from the atmosphere per m<sup>2</sup> daily. Even in winter,  
77 when plants were dormant, it continued to be a CO<sub>2</sub> sink, albeit smaller. Cool temperatures  
78 and high cloud cover inhibit carbon sequestration.

79

80

81

82

## 83 1. Introduction

84

85 Despite their relatively small global footprint of 54,650 km<sup>2</sup> (Mcowen et al., 2017), salt  
86 marshes provide a range of ecosystem services, including shoreline protection (Shepard et al.,  
87 2011), nutrient uptake, nursery grounds for fish populations (Whitfield, 2017) as well as  
88 functioning as significant carbon sinks through CO<sub>2</sub> uptake and storage in their organic rich  
89 sediments (McLeod et al., 2011). These ‘blue carbon’ habitats are recognised for their  
90 significant contribution to the global carbon cycle, as coastal wetlands more broadly are  
91 estimated to have accumulated more than a quarter of global organic soil carbon (Duarte,  
92 2017).

93

94 Saltmarshes are a widely distributed intertidal habitat but are floristically divergent globally  
95 (Adam, 2002), such that commonalities in function and form do not extend across  
96 biogeographic realms. US saltmarshes, for example, are extensively dominated by a single  
97 grassy species, *Spartina alterniflora*, as opposed to the dominance of C<sub>3</sub> Chenopodioideae  
98 species in the southern hemisphere (Adam, 2002). Temperate saltmarshes occupy a  
99 latitudinal range spanning from approximately 30° to 60° (Mcowen et al., 2017) and are most  
100 commonly found along protected coastlines such as bays, estuaries, and lagoons, where they  
101 are sheltered from the full force of wave action (Mitsch and Gosselink, 2000). In the  
102 Southern Hemisphere, temperate saltmarshes have a strong Gondwanan element with high  
103 floristic similarity among the marshes of New Zealand, the southernmost coasts of South  
104 America and South Africa and the southern coastlines of Australia (Adam, 1990). These  
105 marshes are often associated with extensive seagrass meadows and mudflats, and in parts of  
106 their range, mangroves, forming complex coastal mosaics (Huxham et al., 2018).  
107 Saltmarshes have been heavily degraded across their range, and it is estimated that perhaps  
108 up to 50% of the global saltmarsh area has been lost since 1900 (Gedan et al., 2009),  
109 primarily due to land use change.

110

111 In most areas where they occur, seasonality plays a major role in the functioning of temperate  
112 saltmarshes (Ghosh and Mishra, 2017). These ecosystems experience distinct growing and  
113 dormant seasons, primarily driven by temperature, light availability, and precipitation  
114 patterns (Adam, 2000). During the growing season (typically spring and summer), increased  
115 temperatures and longer daylight hours stimulate plant growth, photosynthetic activity, and

116 decomposition processes. Photosynthesis typically outpaces decomposition during this  
117 period, resulting in the temperate saltmarsh acting as a net CO<sub>2</sub> sink (Chmura et al., 2003).  
118 Conversely, the dormant season (usually fall and winter) is characterized by cooler  
119 temperatures and shorter days (Adam, 2000; Howe et al., 2010). These factors lead to  
120 reduced plant growth and photosynthetic activity (Adam, 2000) and while decomposition  
121 processes also slow down due to cooler temperatures, CO<sub>2</sub> release through decomposition  
122 often exceeds CO<sub>2</sub> uptake during this period (Artigas et al., 2015). In Australia, saltmarshes  
123 have been assumed to not exhibit seasonality (Owers et al., 2018) despite there being a  
124 scarcity of data on saltmarsh phenology and the implication this untested assumption could  
125 have on carbon budget estimations.

126

127 Gross primary production (GPP) of saltmarshes is the total amount of CO<sub>2</sub> uptake by plants  
128 through photosynthesis. Respiration (R<sub>e</sub>) leads to a CO<sub>2</sub> flux directed back to the atmosphere  
129 due to all respiration processes occurring within the saltmarsh, involving both autotrophs and  
130 heterotrophs. The difference between these two fluxes is the net ecosystem exchange (NEE).  
131 Saltmarsh ecosystems can act as both sources and sinks of carbon dioxide (CO<sub>2</sub>), influencing  
132 atmospheric CO<sub>2</sub> concentrations (Chmura et al., 2003). However, quantifying their net  
133 exchange remains challenging (Lu et al., 2017) hindering their effective inclusion in Earth  
134 System Models (Ward et al., 2020) and confounding the incorporation of saltmarsh  
135 restoration in emission reduction targets. Eddy covariance (EC) provides a powerful method  
136 for near-continuous, high-frequency monitoring of gas exchange between a vegetated surface  
137 and the atmosphere (Baldocchi, 2003), enabling the determination of net ecosystem exchange  
138 (NEE) of CO<sub>2</sub>, and identifying the forcings that determine how CO<sub>2</sub> fluxes will respond to  
139 global climate change (Borges et al., 2006; Cai, 2011).

140

141 Previous EC studies in coastal saltmarshes have been focused on the Northern Hemisphere, in  
142 sites in the USA (e.g. Hill and Vargas, 2022; Kathilankal et al., 2008; Moffett et al., 2010;  
143 Nahrawi et al., 2020; Schäfer et al., 2019), France (Mayen et al., 2024), Japan (Otani and  
144 Endo, 2019) and China (Wei et al., 2020) but interest in the southern hemisphere is growing  
145 (Bautista et al., 2023). The NEE values from these studies indicate that there is high inter-site  
146 (as well as interannual, Erickson et al., (2013)) variability in carbon dynamics of saltmarshes,  
147 with a link to species types, salinity, hydrology (Moffett et al., 2010; Nahrawi et al., 2020),  
148 site specific biochemical conditions (Seyfferth et al., 2020) and latitude (Feagin et al., 2020).  
149 While generally considered important carbon sinks (e.g. ranging between 130 to 775 g C m<sup>-2</sup>

150 yr<sup>-1</sup> in the USA, according to Kathilankal et al. (2008) and Wang et al.(2016) respectively)  
151 and globally hypothesised to average 382 g C m<sup>-2</sup> y<sup>-1</sup> (Alongi, 2020), some EC studies  
152 revealed saltmarshes to be net sources of CO<sub>2</sub> to the atmosphere (Vázquez-Lule and Vargas,  
153 2021) especially in temperate saltmarshes that experience long dormant periods.

154

155 The aim of this study is to estimate CO<sub>2</sub> and water fluxes in a temperate saltmarsh in  
156 Victoria, southern Australia, to better characterise the effect of seasonality and environmental  
157 variables on the saltmarsh CO<sub>2</sub> budgets. This is the first study in an Australian coastal  
158 saltmarsh where CO<sub>2</sub> fluxes are estimated using the EC method.

159

## 160 2. Methods

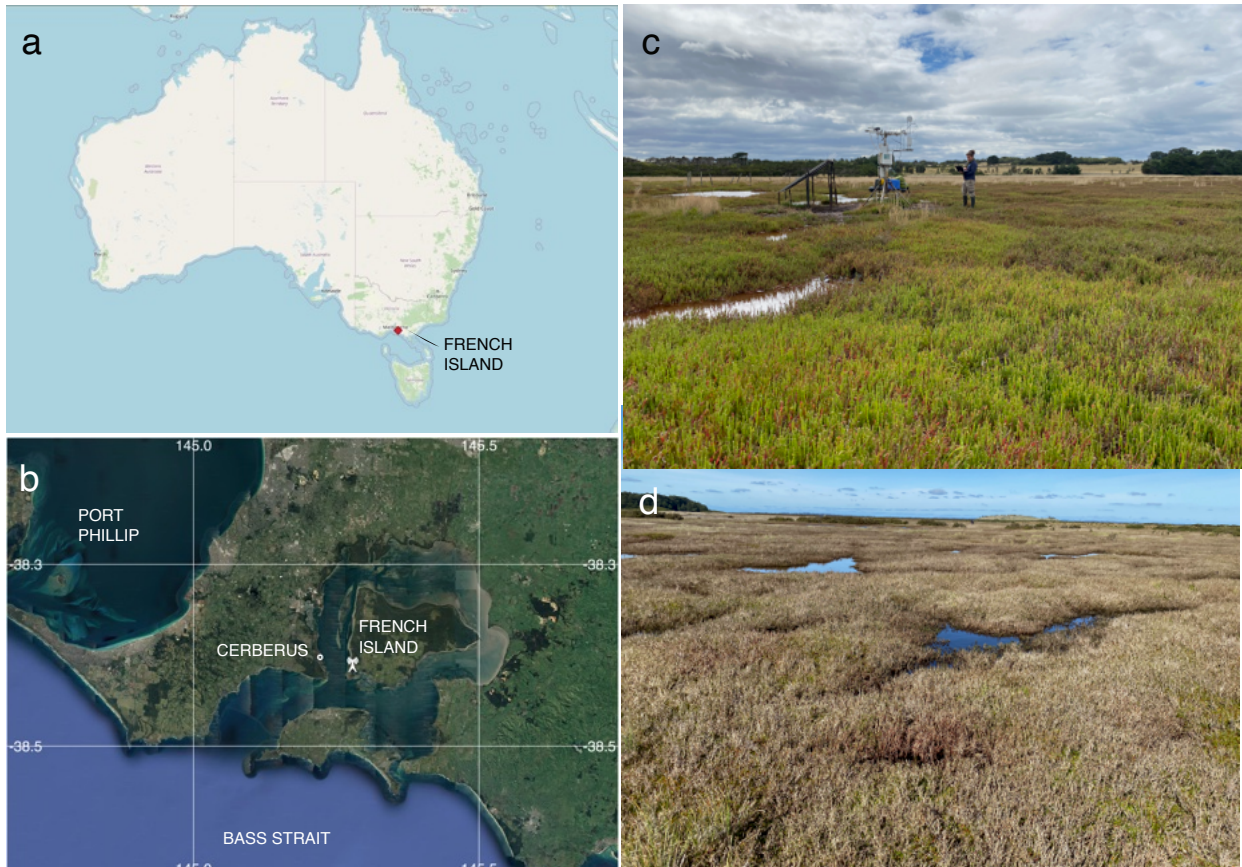
161

### 162 2.1 Site Description

163

164 Ecosystem flux measurements were collected at the Tortoise Head Ramsar coastal wetland on  
165 French Island, Victoria (38.388°S, 145.278°E, Fig. 1) within the Western Port embayment.  
166 French Island is within the Cfb climate zone (temperate oceanic climate) and experiences  
167 distinct seasonal variations in temperature and precipitation. Long term (30 year) climate data  
168 averaged from the nearby Cerberus Station (Australian Bureau of Meteorology, site 86361)  
169 indicated that summers, spanning from December through February, are generally mild to  
170 warm, with maximum temperatures typically ranging from 17°C to 25°C although occasional  
171 heatwaves lead to temporary spikes in temperature that can exceed 30°C. Winters, from June  
172 to September, are cooler, with maximum temperatures ranging between 7°C and 14°C and a  
173 mean minimum temperature of 6°C. Frost is infrequent due to maritime influence, though  
174 crisp mornings below 0°C occur 10% of the time in winter. Rainfall, evenly distributed  
175 throughout the year, averages ca. 715 mm y<sup>-1</sup>, although in 2020 the site had higher than  
176 average rainfall (860 mm y<sup>-1</sup>). The island is exposed to weather patterns influenced by the  
177 Southern Ocean and Bass Strait, leading to occasional storm systems, particularly in winter,  
178 bringing gusty winds and increased precipitation. Western Port has semi-diurnal tides with a  
179 range of nearly 3 m, resulting in wide intertidal flats occupied by mangroves of the species  
180 *Avicennia marina* and saltmarshes. The saltmarsh in this study experiences complex  
181 hydrological conditions, and we found that inundation does not directly link to tides.

182



183

184

185 Figure 1: a) The location of French Island along the Bass Strait coast of Australia, and b) The  
 186 location of the flux tower on French Island as well as the nearby Cerberus meteorological  
 187 station (Bureau of Meteorology, Australia), © Google Earth. c) An image of the saltmarsh  
 188 within the flux tower footprint during the growing season (with the tower and the author in  
 189 the background), taken in February 2020 by Prudence Perry. d) an image of the saltmarsh  
 190 during the dormant period, taken at the same location in September 2020 by Ruth Reef.

191

192 The site at French Island is dominated by an extensive temperate coastal saltmarsh  
 193 community that is a particularly good natural representation of a broader biogeographic  
 194 saltmarsh grouping which covers an area of ca. 7000 ha along Victoria's central coast  
 195 embayments (Navarro et al., 2021). While the wetland at the site is a saltmarsh-mangrove-  
 196 seagrass wetland system, the footprint of the flux tower was limited to the saltmarsh alone,  
 197 which extends more than a kilometre from the shoreline in places. This geography provided  
 198 the critical horizontally homogenous area with flat terrain required for ecosystem flux  
 199 measurements. Floristically this saltmarsh is species poor, dominated by *Sarcocornia*  
 200 *quinqueflora*. Stands of *Tecticornia arbuscula* are common in this saltmarsh, while *Atriplex*  
 201 *cinerea* approx. 7% Australia and *Distichis distichophylla* can be prevalent depending on

202 elevation and soil drainage conditions. *Sarcocornia quinqueflora* is a perennial succulent and  
203 at the temperate ranges of its distribution it has a distinct growing season from October to  
204 May (Fig. 1c) when the stems turn red, followed by a woody and fibrous dormant period  
205 during the colder months of June through September (Fig. 1d). The height of the dominant  
206 vegetation ranged between 0.3 m.

207

## 208 2.2 Data Collection and Analysis

209

210 Eddy covariance measurements were made between November 2019 and August 2021  
211 capturing both the saltmarsh growing season (October-May) as well as a dormant period  
212 (June-September). An array of standard micro-meteorological instruments included a 3-  
213 dimensional sonic anemometer (CSAT3, Campbell Scientific, USA), an open-path infra-red  
214 carbon dioxide (CO<sub>2</sub>) gas and water vapour (H<sub>2</sub>O) analyser (Li-7500, Li-Cor, USA) and 2  
215 data-loggers. The tower was powered by a solar array with two accompanying 12V DC  
216 storage batteries. The sonic anemometer was mounted 2.3 m above ground. The CO<sub>2</sub>/H<sub>2</sub>O  
217 gas analyser was mounted 0.11 m longitudinally displaced from the anemometer. A CR3000  
218 datalogger (Campbell Scientific, USA), recorded the Li-7500, anemometer, short- and long-  
219 wave radiation (CNR4, Klip & Zonen, the Netherlands), air temperature and humidity (083E,  
220 Met One, USA) readings at 10 Hz frequency. Due to the location of the site in the Bass Strait  
221 (a region that experiences regular winter storms, high wind speeds and higher than national  
222 average cloud cover) the tower sustained damage due to winter storms several times during  
223 the deployment, as well as suffered periods of poor power supply due to short day lengths  
224 and high cloud cover; this was exacerbated by poor accessibility to the remote location during  
225 COVID-19 travel restrictions. The analysis thus focused on extended periods of continuous  
226 daily records and periods with large gaps in the dataset were removed.

227

228 Ecosystem fluxes were calculated for 30 min intervals using Eddy Pro software v.7 (LI-COR  
229 Inc., USA) Express Mode protocols (see settings at  
230 <https://www.licor.com/env/support/EddyPro/topics/express-defaults.html>). This processing  
231 step includes coordinate axis rotation correction, trend correction, data synchronisation,  
232 statistical tests for quality, density corrections and spectrum corrections. As part of this step,  
233 flux quality flags were assigned to the calculated CO<sub>2</sub> fluxes using the 0–2 flag policy  
234 ‘Mauder and Foken 2004’, based on the steady state test and the developed turbulent



235 conditions test. The steady state test checks if fluxes remain consistent over the 30-minute  
 236 averaging period by comparing the mean and standard deviation (SD) of fluxes in the first  
 237 and second halves of the period. The developed turbulent conditions test ensures turbulence is  
 238 well-developed and its energy spectra fits the Kolmogorov spectrum. Both tests assign partial  
 239 flags that are combined into a single flag (0–2) in Eddy Pro, indicating the overall data  
 240 quality. Only data that met the criteria of being in quality class 0 (‘best quality fluxes’) for  
 241 CO<sub>2</sub> flux were chosen for further analysis. We further removed anomalous data points  
 242 defined as values that exceed four SDs from the mean CO<sub>2</sub> flux; this resulted in the additional  
 243 loss of ca. 1% of the dataset. Gap filling was not applied. Additional filtering was applied to  
 244 nighttime data due to known weak convection at night, thus CO<sub>2</sub> flux data during periods of  
 245 atmospheric stability, i.e. when night friction wind velocities ( $u^*$ ) were below 0.2 m s<sup>-1</sup>, were  
 246 excluded following inspection of the nightly NEE vs.  $u^*$  curve to detect the threshold where  
 247 NEE fall-off occurs (i.e. the Change Point Detection method, Barr et al., 2013). This resulted  
 248 in a dataset of 674 day-time and 606 nighttime flux measurements during the dormant period  
 249 and 4124 day-time and 3020 nighttime flux measurements for the growing period (Table 1).  
 250 The growing season dataset included 90 days with 85% or more flux data coverage, while the  
 251 dormant season dataset included 18 days, and these days were used for 24-hour flux  
 252 integrations.

253

254 Table 1: Mean ( $\pm$ SD) net ecosystem exchange ( $\mu\text{mol CO}_2 \text{ m}^{-2} \text{ s}^{-1}$ ) during day- and nighttime  
 255 respectively, as well as the corresponding number of half hourly measurements from each  
 256 month, following filter applications (n).

257

Month	Daytime Mean NEE (SD); n	Nighttime Mean NEE (SD); n	Season
October 2019	-2.29 (3.08); 121	2.04 (1.28); 70	Greening up
November 2019	-1.84 (3.89); 151	2.85 (1.75); 110	Greening up
December 2019	-3.33 (4.59); 96	1.14 (1.70); 15	Growing
January 2020	-1.31 (3.31); 63	2.10 (0.79); 27	Growing
February 2020	-3.83 (4.11); 540	1.89 (1.10); 280	Growing
March 2020	-3.86 (3.90); 494	1.63 (0.78); 351	Growing
August 2020	0.05 (2.05); 150	1.76 (1.22); 39	Dormant
September 2020	-0.98 (2.04); 147	1.27 (0.96); 101	Dormant
January 2021	-4.81 (5.04); 602	2.15 (1.55); 373	Growing
February 2021	-3.62 (4.27); 615	2.00 (1.19); 423	Growing
March 2021	-3.07 (3.95); 660	1.76 (1.20); 556	Growing

April 2021	-2.08 (3.02); 409	1.15 (0.87); 403	Growing
May 2021	-0.98 (2.57); 377	1.14 (1.04); 423	End of Growing
June 2021	0.58 (1.67); 271	0.93 (1.30); 328	Dormant
July 2021	1.07 (1.38); 102	0.82 (0.62); 127	Dormant

258

259

260 Half-hourly average CO<sub>2</sub> flux was measured in  $\mu\text{mol m}^{-2} \text{s}^{-1}$ , with positive fluxes indicating a  
 261 flux direction from the Earth's surface to the atmosphere. Net ecosystem exchange (NEE)  
 262 was defined as the net flux of CO<sub>2</sub> from the atmosphere to the marsh and was often negative  
 263 during daytime, indicating that Gross Primary Productivity (GPP) was larger than ecosystem  
 264 respiration ( $R_e$ ). Evapotranspiration (ET) was calculated by Eddy Pro as the ratio between the  
 265 latent heat flux (LE) and latent heat of vaporisation ( $\lambda$ ). Ecosystem water use efficiency  
 266 (WUE<sub>e</sub>) was then expressed as the ratio between daytime net ecosystem productivity in g  
 267 CO<sub>2</sub> m<sup>-2</sup> h<sup>-1</sup> and evapotranspiration in mm h<sup>-1</sup>.

268

269 A two-dimensional footprint estimation was provided according to the simple footprint  
 270 parameterisation described in Kljun et al. (2015) calculating the ground position of the  
 271 cumulative fraction of flux source contribution by distance for each 30-minute interval. We  
 272 assessed the short-term effects of environmental factors on CO<sub>2</sub> fluxes at a half-hourly time  
 273 scale (e.g. the effects of light, air temperature and vapour pressure deficit) using a series of  
 274 non-linear or linear models. These analyses were limited to the growing season, when the  
 275 plants were actively photosynthesising. To calculate the daily-integrated CO<sub>2</sub> and H<sub>2</sub>O fluxes,  
 276 the daily sum of these fluxes was determined for days with at least 85% data coverage. This  
 277 involved using the trapezoid rule to estimate the area under the curve for each of these 24-  
 278 hour periods. The trapezoid rule approximates the total flux by dividing the day into smaller  
 279 intervals, each lasting 1,800 seconds (30 minutes). For each data interval, the area is  
 280 calculated by averaging the flux values at the beginning and end of the interval, then  
 281 multiplying by the interval duration. These areas are then summed to obtain the total daily  
 282 flux. This method ensures that even with some missing data points, a reliable estimate of the  
 283 daily flux can be obtained. All post-processing and statistical analyses were performed in R  
 284 4.3.2 (R Core Team, 2024) including the packages *ggplot2*, *clifro*, *MASS*, *dismo*, *amerifluxr*,  
 285 *rmarkdown*, *geosphere*, *ggmap* and *gbm*.

286

287 For the CO<sub>2</sub> budget, Net Ecosystem Production (NEP), was defined as NEP=-NEE.  
288 Nighttime NEE is referred to as R<sub>e</sub> and was corrected for temperature effects on respiration  
289 using an exponential Arrhenius-type relationship (Lloyd and Taylor, 1994).

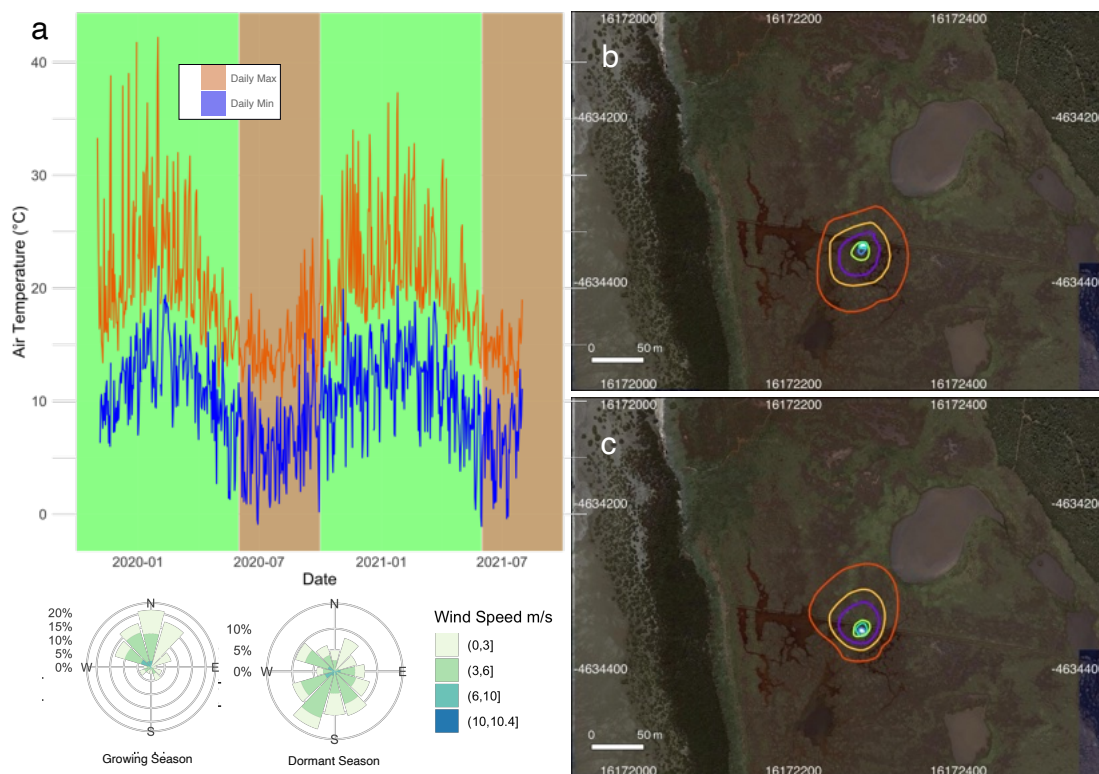
290

### 291 3 Results

292

293 The observations were divided into a growing season and a dormant season to reflect the  
294 seasonal phenology of the dominant vegetation type within the flux tower footprint. During  
295 the growing season, mean temperature averaged 22.3°C. Several heatwaves occurred during  
296 this period, with temperatures exceeding 40°C on a few occasions in 2019. The dormant  
297 season was significantly colder and windier, with frequent southerly winds (Fig. 2a).

298 Footprint models showed a slight variation in flux source between the two seasons, although  
299 in both cases the size of the footprint and the vegetation composition within the footprint was  
300 similar (Figs. 2b and 2c), but the shape was skewed to the north during winter due to the  
301 prevalent southerly winds in that season (Fig. 2a). 70% of the flux measurement source was  
302 from within 50 m of the tower, while the maximum length of the source location was 73 m.



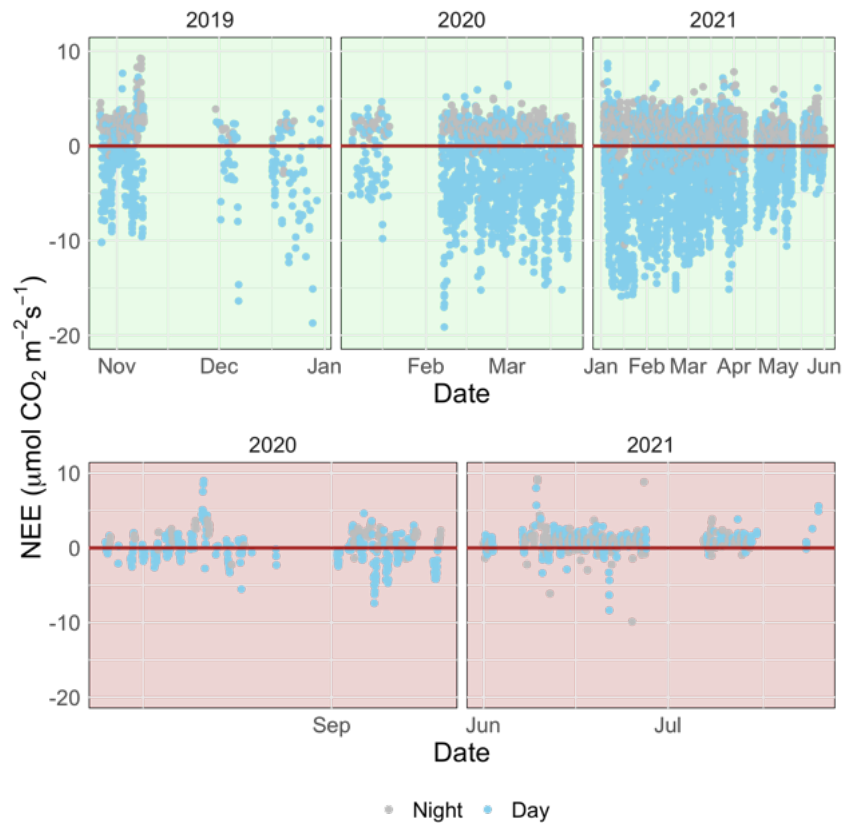
303

304

305

306 Figure 2: a) The minimum and maximum daily temperature recorded at the Cerberus  
307 meteorological station (Bureau of Meteorology, Fig. 1b) during 2019-2021. The marsh  
308 growing (October-May) and dormant (June-September) periods are shaded in green and pink  
309 respectively. A corresponding wind rose diagram summarises the wind speeds and directions  
310 measured at the tower site during the observation periods. The flux source footprint  
311 surrounding the tower during the dormant season (b) and the growing season (c) shows the  
312 cumulative flux source contribution to the flux measurements, with the outer red line  
313 representing the distance by which 90% of the calculated flux is sourced and the other  
314 isolines from the tower outwards correspond to 10%, 20%, 40%, 60% and 80% of the flux.  
315

316 The growing season dataset included 90 days with 85% or more flux data coverage, while the  
317 dormant season dataset included 18 days. There was a strong temporal variability in net  
318 ecosystem exchange (NEE) across both short (daily) and long (seasonal) temporal scales  
319 (Fig. 3). Daytime fluxes were defined as flux points where the global radiation values in the  
320 flux averaging half-hour interval were  $>12 \text{ W m}^{-2}$  (as per EddyPro methodology). At the  
321 diurnal scale, saltmarsh NEE were negative mostly during the day and positive mostly during  
322 the night and ranged between  $-19.1$  and  $10.86 \mu\text{mol m}^{-2} \text{ s}^{-1}$  across the measurement periods.  
323 Monthly averages and data coverage are shown in Table 1.



325

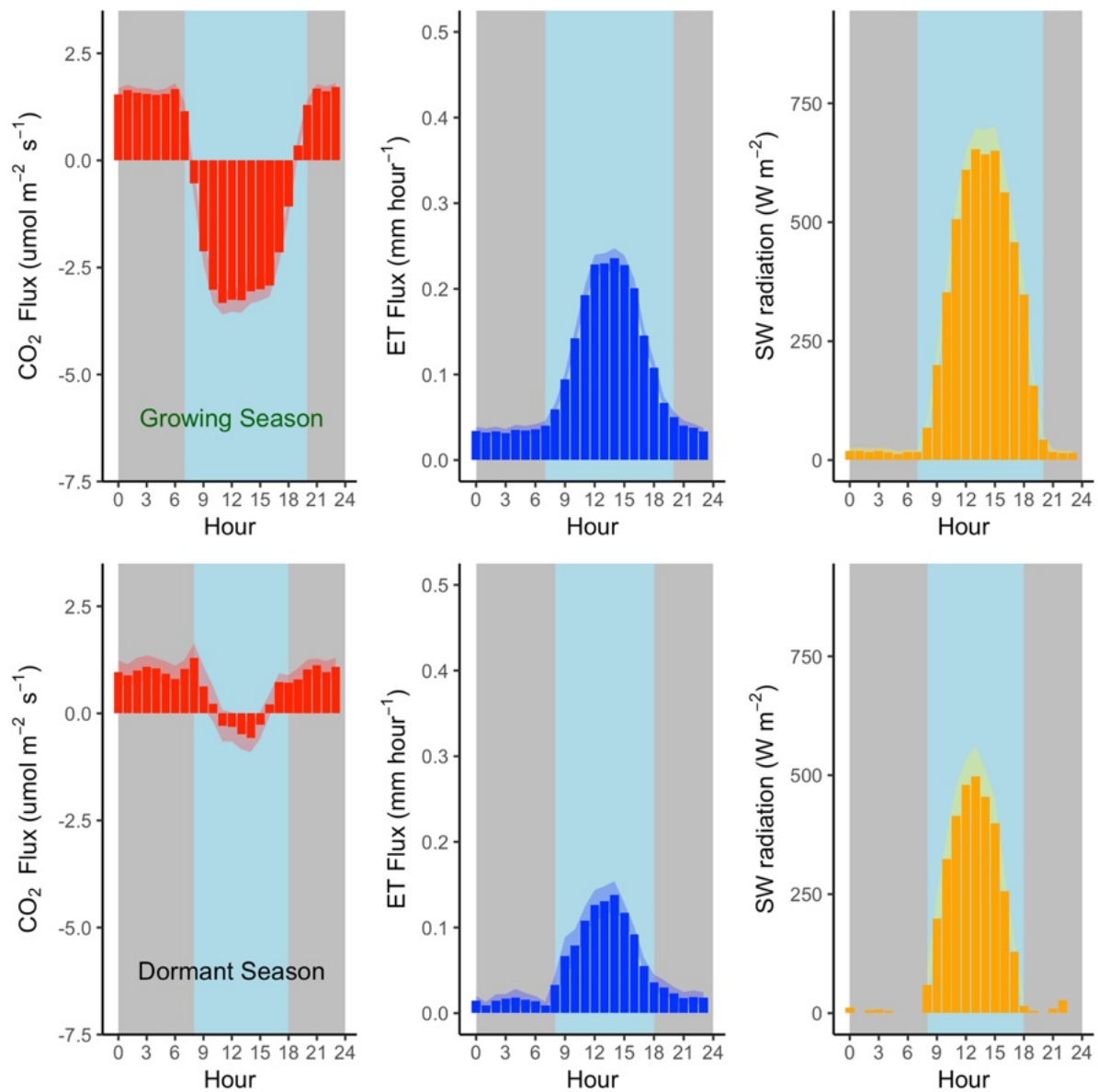
326 Figure 3: A time series of half-hourly measurements of CO<sub>2</sub> flux between a temperate  
 327 saltmarsh and the atmosphere measured by eddy covariance during the marsh growing season  
 328 (top) and the dormant season (bottom). Blue and grey points indicate measurements taken  
 329 during daytime and nighttime respectively. Positive fluxes indicate a direction of flux from  
 330 the Earth surface to the atmosphere.

331

332 Flux rates varied across the day, with CO<sub>2</sub> uptake peaking at 11:00 during the growing  
 333 season, and later in the day (14:00) during the dormant period (Fig. 4). Ecosystem respiration  
 334 rates ( $R_e$ , defined as nighttime CO<sub>2</sub> flux) were on average ( $\pm$ SD) 1.77 ( $\pm$ 1.12)  $\mu\text{mol m}^{-2} \text{s}^{-1}$   
 335 during the growing season and 1.0 ( $\pm$  0.93)  $\mu\text{mol m}^{-2} \text{s}^{-1}$  during the dormant period. The  
 336 difference in ecosystem respiration between the growing and dormant seasons is highly  
 337 significant (t-test,  $p < 0.01$ ). Daytime CO<sub>2</sub> flux was on average ( $\pm$ SD) -3.53 ( $\pm$  4.15)  $\mu\text{mol m}^{-2}$   
 338  $\text{s}^{-1}$  during the growing season and -0.25 ( $\pm$  2.18)  $\mu\text{mol m}^{-2} \text{s}^{-1}$  during the dormant season.  
 339 Thus, we derive that the maximum Gross Primary Productivity (GPP) of this ecosystem from  
 340 NEE and temperature-corrected  $R_e$  (Fig. 5), measured during the growing season, is ca. -5.34  
 341  $\pm$  4.3  $\mu\text{mol CO}_2 \text{ m}^{-2} \text{ s}^{-1}$  (-5.53  $\pm$  4.45  $\text{g C m}^{-2} \text{ day}^{-1}$ ). Average  $R_e$  is thus estimated to comprise  
 342 33% of GPP.

343

344 Mean ( $\pm$ SD) daily evapotranspiration was 2.48 mm ( $\pm$ 2.79 mm) during the growing season  
345 and 0.97 mm ( $\pm$ 1.35 mm) during the dormant season (Fig. 4). Evapotranspiration peaked at  
346 noon AEST during the growing season (0.26 mm h<sup>-1</sup>), and later in the day (14:00 AEST)  
347 during the dormant season (0.14 mm h<sup>-1</sup>).  
348



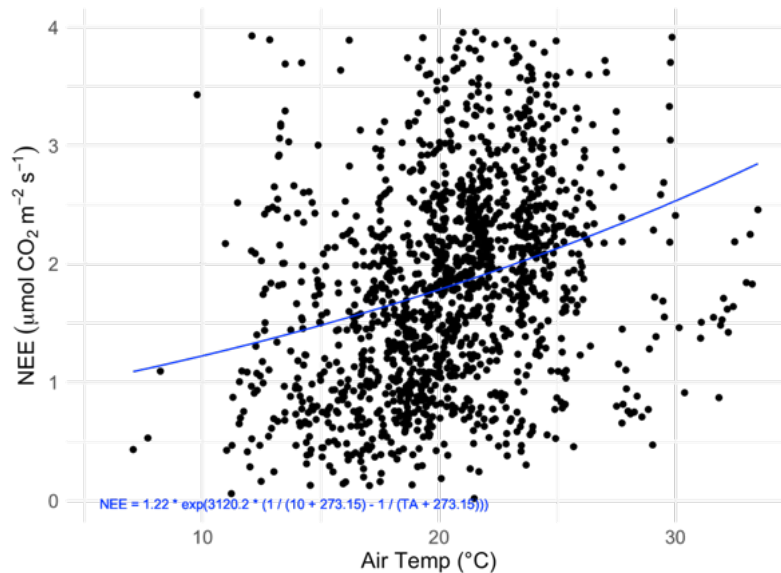
349

350

351 Figure 4: Mean hourly CO<sub>2</sub> and H<sub>2</sub>O flux (evapotranspiration) rates during the growing  
352 season (top) and the dormant season (bottom) alongside mean short wave incoming radiation.

353 Shading corresponds to 1 standard deviation (SD) around the mean. Grey plot background

354 approximates nighttime periods, while light blue approximates daytime (actual day length  
355 varies within each season).  
356



357  
358 Figure 5: The relationship between nighttime half-hourly flux measurements (NEE) taken  
359 between the hours of 22:00 and 02:00 and air temperature (TA). The fitted curve (blue line) is  
360 the fitted Lloyd & Taylor Arrhenius non-linear model:  $NEE = 1.22 * \exp(3120.2 * (1 / 283.2 -$   
361  $1 / (TA + 273.2)))$ ,  $R^2 = 0.09$ .

362  
363 The effect of some environmental forcings on daytime NEE during the saltmarsh growing  
364 season were explored (Fig. 6). To distinguish this daytime-only value from the 24-hour  
365 carbon balance integration, and to better highlight CO<sub>2</sub> uptake, NEP values are shown.

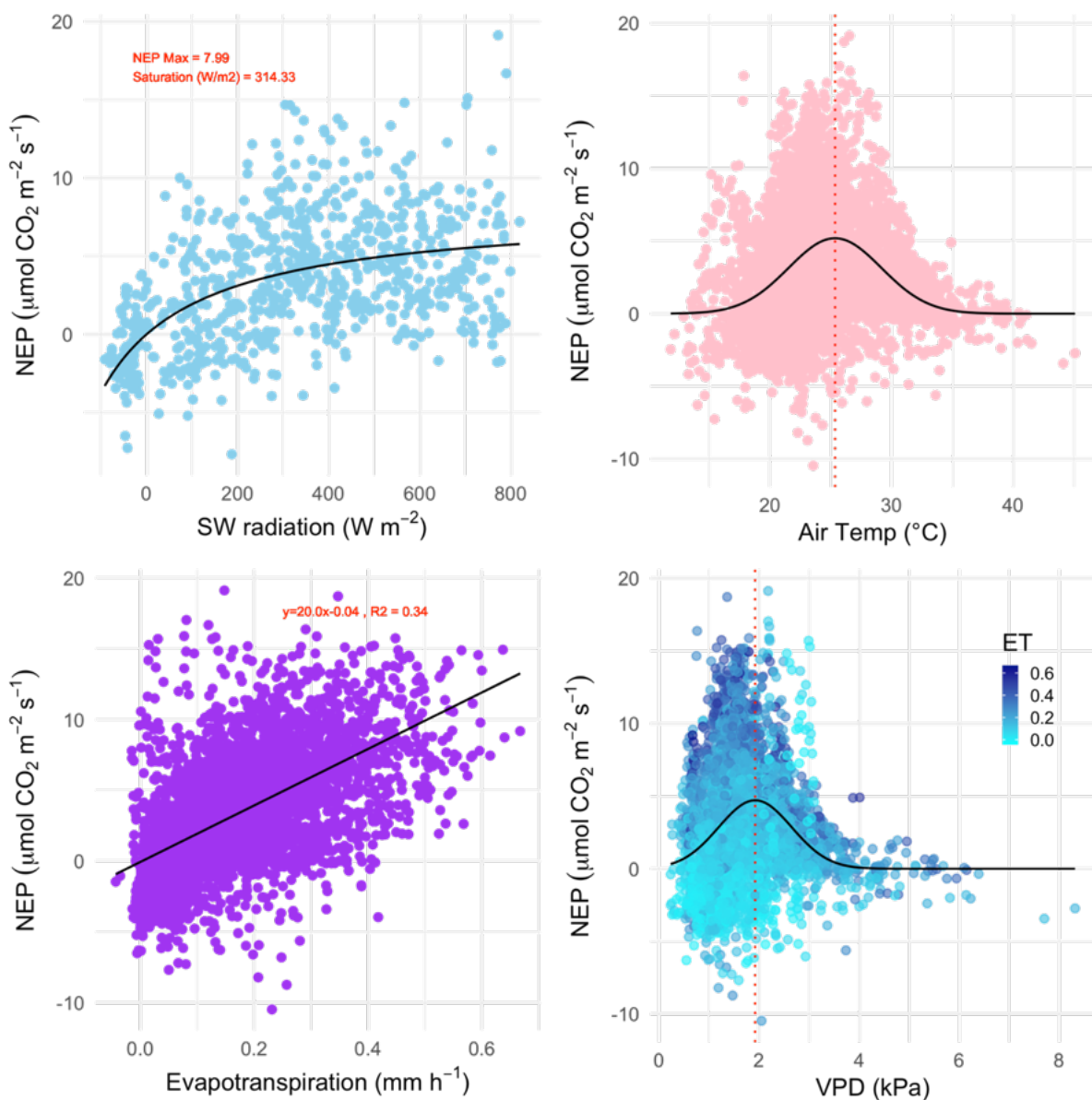
366  
367 Short wave radiation (visible light) was a limiting factor to NEP below approximately 300 W  
368 m<sup>-2</sup>, but radiation did not reach damaging levels that would lead to a drop in NEP throughout  
369 the measurement range, which reached a maximum level of ca. 800 W m<sup>-2</sup>. Unlike light, the  
370 NEP-air temperature relationship followed a Gaussian response, with the highest NEP  
371 achieved at the optimal temperature of 25.3°C with a SD of 3.8°C followed by a decline in  
372 CO<sub>2</sub> uptake by the marsh at higher temperatures. The minimum and maximum air  
373 temperatures for which modelled NEP nears zero (defined here as 3 SDs from the mean) are  
374 13.9°C and 36.7°C respectively. Temperature also had a slight but significant positive linear

375 relationship with ecosystem respiration (slope=0.07  $\mu\text{mol CO}_2 \text{ m}^{-2} \text{ s}^{-1} \text{ }^\circ\text{C}^{-1}$ ,  $p < 0.01$ , data not  
376 shown).

377

378 NEP was positively correlated with evapotranspiration during the growing season (Pearson  $r$   
379 = 0.59, Fig.6 C). The slope of the NEP/ET relationship was 20.0, indicating an ecosystem  
380 water use efficiency ( $\text{WUE}_e$ ) of 0.86  $\text{g C kg}^{-1} \text{ H}_2\text{O}$  ( $R^2 = 0.34$ ,  $p < 0.001$ ). The response of  
381 NEP to atmospheric vapour pressure deficit (VPD) fit a Gaussian relationship (the commonly  
382 observed inverse U-shaped curve relationship in response to VPD in plants), with NEP  
383 declining rapidly when VPD exceeded 2.39 kPa. The optimal range of VPD within which  
384 NEP was maximised in this ecosystem was 1.92 kPa ( $\pm 0.73$  kPa).

385



386



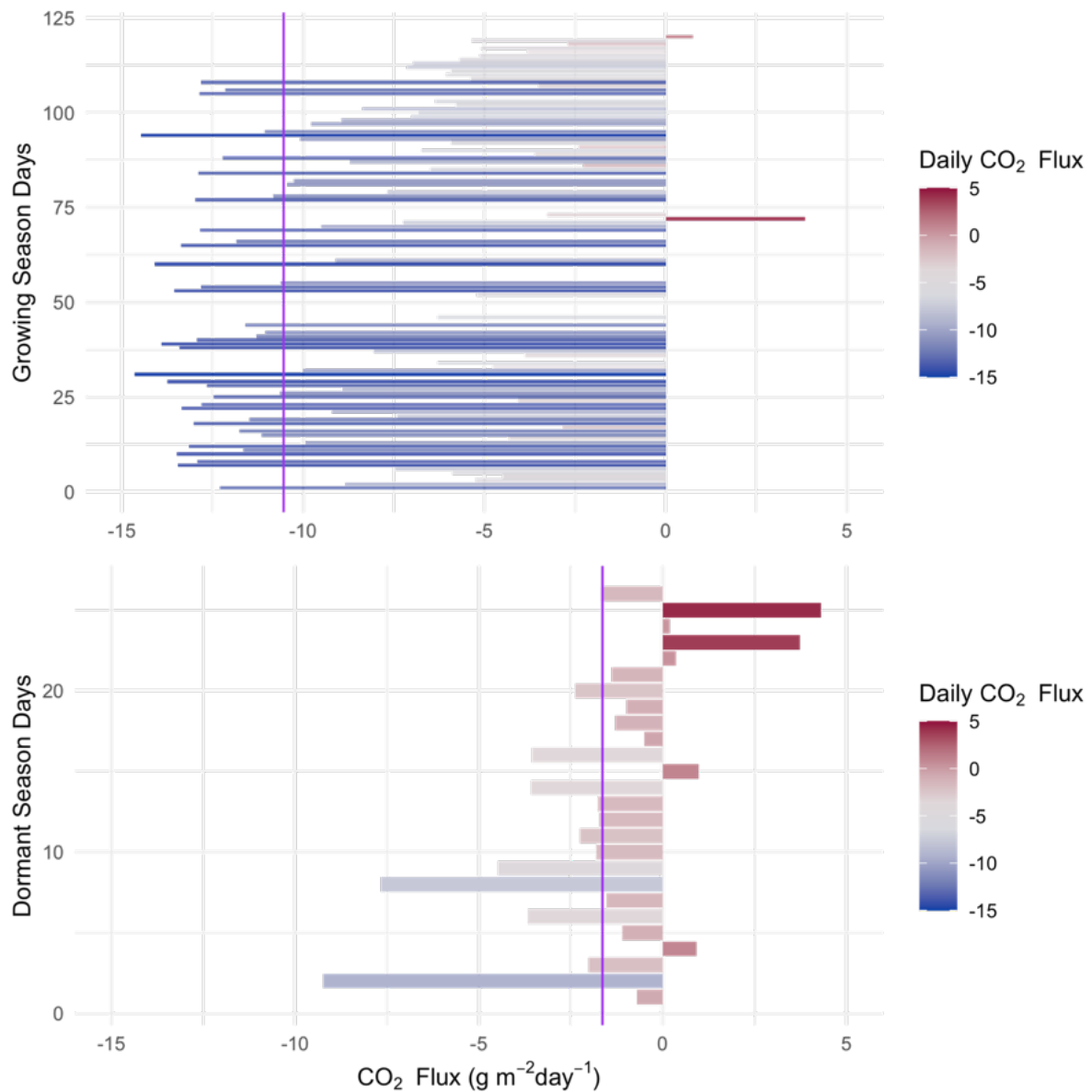
387 Figure 6: The relationship between growing season daytime half-hourly values of net  
388 ecosystem productivity (NEP,  $\mu\text{mol CO}_2 \text{ m}^{-2} \text{ s}^{-1}$ ) and corresponding environmental variables.  
389 a) Net shortwave (SW) radiation (visible light); black line is the Michaelis-Menten model of  
390 best fit. The coefficient of saturation is at  $314 \text{ W m}^{-2}$  and maximum net productivity is  $8.0$   
391  $\mu\text{mol CO}_2 \text{ m}^{-2} \text{ s}^{-1}$ . b) Air temperature (TA); black line is a Gaussian model of best fit with a  
392 temperature optimum at  $25.3^\circ\text{C}$ . c) Evapotranspiration; linear model ( $R^2 = 0.34$ ) has a slope  
393 of  $20.0$ . d) Vapour Pressure Deficit; black line is a Gaussian model of best fit with a VPD  
394 optimum at  $1.92 \text{ kPa}$ , points are coloured by the level of evapotranspiration during the half  
395 hourly NEP measurement.

396

397 When integrated over a 24-hour period, the saltmarsh is on average a daily  $\text{CO}_2$  sink during  
398 all canopy phenological phases (Fig. 7), although during the dormant season the sink is  
399 weaker, with an average uptake of  $-2.42 \text{ g CO}_2 \text{ m}^{-2} \text{ day}^{-1}$  ( $\pm 2.54$ ). During the growing season  
400 (defined as the non-dormant period and thus reflecting several phenological stages), the  
401 marsh is a substantial sink with a mean ( $\pm\text{SD}$ ) daily NEP of  $10.95 \text{ g CO}_2 \text{ m}^{-2} \text{ day}^{-1}$  ( $\pm 4.98$ )  
402 over a 24-hour period (ranging between  $-22.8$  and  $4.3 \text{ g of CO}_2 \text{ emission to the atmosphere}$   
403  $\text{m}^{-2} \text{ day}^{-1}$ ). The daily  $\text{CO}_2$  budget during the growing season showed some variability among  
404 days ( $\text{CV}=0.46$ , Fig. 7) and days with lower average light levels (i.e. cloudy days) had a  
405 significant negative impact on the  $\text{CO}_2$  budget (multiple linear regression,  $p < 0.02$ ,  $R^2 =$   
406  $0.27$ ). Daily maximum air temperatures did not have a significant impact on the daily  $\text{CO}_2$   
407 budget ( $p = 0.77$ ) at this location, although NEE was significantly affected by temperature at  
408 finer temporal scales (Figure 6).

409

410



411

412 Figure 7: Daily (24 h) integrated NEE in  $\text{g CO}_2 \text{ m}^{-2} \text{ day}^{-1}$  during the saltmarsh growing  
 413 season (top) and the dormant season (bottom) for days with data density  $> 85\%$ . Purple lines  
 414 indicate the mean daily integrated flux for each season ( $-10.54$  and  $-1.64 \text{ g CO}_2 \text{ m}^{-2} \text{ day}^{-1}$  with  
 415 an SD of  $4.98$  and  $2.54$  for growing and dormant respectively). A positive balance indicates  
 416 an integrated net flux of  $\text{CO}_2$  from the Earth's surface to the atmosphere over the 24-hour  
 417 period.

418

419

420 4 Discussion

421

422 The study provided high-frequency measurements of an abundant greenhouse gas (CO<sub>2</sub>)  
423 using a precise technique (eddy covariance flux) in an ecosystem with limited historical  
424 measurements. Time series analysis was performed on CO<sub>2</sub> flux measurements across various  
425 scales (daily, nightly, diel, half-hourly, hourly, seasonally) to assess the impacts of ET, SW  
426 radiation, VPD, and TA on CO<sub>2</sub> flux and how these relationships change throughout the year.  
427 Seasonality was observed for the first time in an Australian saltmarsh and had a significant  
428 effect on carbon and water flux. Growing season net ecosystem productivity was five times  
429 greater than during the dormant period. Seasonality in Australian marshes has not been  
430 previously reported in the scientific literature and contradicts previous assumptions that  
431 Australian saltmarshes do not exhibit the growing and dormant phenology observed on other  
432 continents (Clarke and Jacoby, 1994). Seasonality had a significant impact on the daily  
433 carbon fluxes in this marsh and is an important characteristic of this habitat that has been  
434 overlooked (Owers et al., 2018). Seasonality can also have other broader implications yet to  
435 be considered in Australian marshes. For example, in the USA, the saltmarsh greening up  
436 period was shown to be an important range-wide timing event for migratory birds (Smith et  
437 al., 2020) with plant-growth metrics predicting the timing of nest initiation for shorebirds.  
438 Saltmarshes in Australia are important roosting and feeding sites along the East Asian  
439 Australasian Flyway, particularly for waders, thus potentially a similar relationship between  
440 migration timing and saltmarsh phenology could be occurring. Seasonality also affects other  
441 significant ecosystem functions such as the bio-geomorphological feedback between  
442 saltmarshes, coastal hydrodynamics and landscape evolution (Reents et al., 2022).

443

444 We derived the light-response and associated coefficients of light regulation of saltmarsh  
445 NEE using the Michaelis-Menten model (Chen et al., 2002). Quantum (or production)  
446 efficiency is the predominant input in remote sensing techniques to model productivity, and is  
447 specific to the biome (Hilker et al., 2010). While not directly comparable to leaf level  
448 quantum efficiency measurements, the quantum efficiency ( $\alpha$ ) of the NEP light response  
449 curve was estimated from the slope of the Michaelis-Menten model to be 0.025  $\mu\text{mol CO}_2 \text{ J}^{-1}$ .  
450 The ecosystem reached light saturation at an insolation of 314  $\text{W m}^{-2}$ , but daytime insolation  
451 was below this value more than 50% of the time suggesting that light might be a significant  
452 limiting factor to NEP at this marsh, especially during winter. The level of light limitation we  
453 observed is an underestimation, due to the loss of high-quality EC data during periods of rain.  
454 The solar geometry at this latitude and the length of day result in an annual average top of

455 atmosphere SW radiation of  $250 \text{ W m}^{-2}$ , but clouds can strongly modulate the SW radiation  
456 balance (SWCRE), and apart from the months of January and February when cloudy days are  
457 less frequent (10-12 days per month), cloudy days are frequent at this site, averaging 15-17  
458 days per month (Bureau of Meteorology) and could significantly impact on NEP.

459

460 Temperature is another forcing that significantly impacts NEE at this marsh, with an optimal  
461 range for maximum NEP at  $25.3^{\circ}\text{C}$  ( $21.5^{\circ}\text{C}$ - $29.1^{\circ}\text{C}$ ). Data for Australian saltmarshes is not  
462 available, but this optimal temperature response range is similar to that measured  
463 experimentally in a saltmarsh species in an equivalent climate zone (e.g. Georgia,  
464 (Giurgevich and Dunn, 1981)) and to the values hypothesised for the habitat from data  
465 collected along the US Atlantic Coast, (Feher et al., 2017). The long-term average maximum  
466 daytime temperature at this site is  $19.2^{\circ}\text{C}$ , which is cooler than the optimal range for NEE  
467 suggesting temperature can be a significant limiting factor to productivity, especially during  
468 the dormancy period where average monthly maximum temperatures are only  $13.7^{\circ}\text{C}$  to  
469  $16.6^{\circ}\text{C}$  (Bureau of Meteorology). During the growing season the average maximum  
470 temperatures are within the range of optimal NEE ( $20.6^{\circ}\text{C}$  to  $23.1^{\circ}\text{C}$ ), although hot days  
471 ( $>30^{\circ}\text{C}$ ) significantly depress NEE and depending on the year, can be common during  
472 summer months (averaging 2-6 days per month). Within the diversity of saltmarsh species  
473 found globally, some species have C4 photosynthetic pathways (Drake, 1989). C4  
474 photosynthesis plants often exhibit higher optimum temperature ranges ( $30$ - $35^{\circ}\text{C}$ , Berry and  
475 Björkman, 1980) than C3 photosynthesis plants ( $20$ - $25$ ), and the cooler conditions at this site  
476 could explain the absence of C4 plants from this bioregion. The parabolic relationship  
477 between NEP and air temperature and NEP and VPD suggest that higher air temperatures and  
478 VPD (which are expected with climate change) could negatively impact  $\text{CO}_2$  uptake by these  
479 coastal ecosystems. High VPD was related to lower NEP, and to a lesser extent, lower ET  
480 (Fig. 6d). However, VPD increases atmospheric demand for water, increasing the evaporation  
481 from the saturated marsh surfaces in the footprint, and this atmospheric demand could be  
482 forcing ET at high VPD rather than plant moderation via reduced transpiration, even if  
483 transpiration is reduced. Thus, despite maintained ET during VPD periods we cannot  
484 conclude a non-closure of stomata. NEP also reduced below a VPD of  $1.92 \text{ KPa}$ , but at our  
485 field site low VPD correlated with low temperatures ( $r = 0.88$ ), and low temperatures were  
486 shown to limit NEP.

487

488 In saltmarshes, evapotranspiration occurs from plant mediated transpiration but also from soil  
489 pores (which tend to be saturated), wetted leaves and open water. We observed average  
490 evaporation rates of 2.48 mm day<sup>-1</sup> during the growing season and 0.97 mm day<sup>-1</sup> during the  
491 dormant season. Actual evapotranspiration in this region modelled using the CMRSET  
492 algorithm is estimated to range between 0.6 and 3.2 mm day<sup>-1</sup> during winter and summer  
493 respectively (McVicar et al., 2022); our field measurements support the model. Overall,  
494 rainfall is in excess of the requirements for maintaining ET at this site, although deficits can  
495 develop for short periods during the growing season, when ET is higher, perhaps explaining  
496 the drier saltmarsh surface during this period. Conversely, long term rainfall excess could be  
497 contributing to the complicated hydrology at this location, where inundation is not strictly  
498 associated with tidal stage (data not shown) and our observation of long (5-day) periods of  
499 inundation during winter.

500

501 Growing season ET rates are significantly higher than those of the dormant season, partly due  
502 to the solar configuration in winter as opposed to summer, but also due to phenological  
503 changes. A big leaf model estimation of evapotranspiration from saltmarshes in New South  
504 Wales estimates ET to be highly sensitive to vegetation height, increasing by more than 1 mm  
505 day<sup>-1</sup> as vegetation height increases from 0.1 to 0.4 m (Hughes et al., 2001) and transpiration  
506 in saltmarsh plants in the cold season has been shown to account for only 20% of the annual  
507 transpiration budget (Giurgevich and Dunn, 1981) following the same pattern as the seasonal  
508 distribution of productivity.

509

510 The rate of carbon uptake per unit of water loss (WUE) is a key ecosystem characteristic,  
511 which is a result of a suite of physical and canopy physiological forcings, and has direct  
512 implications for ecosystem function and global water and carbon cycling. Mean water use  
513 efficiency (WUE<sub>e</sub>) of this saltmarsh was estimated at 0.86 g C kg<sup>-1</sup> H<sub>2</sub>O, which is markedly  
514 lower than for grass dominated saltmarshes in China (2.9 g C kg<sup>-1</sup> H<sub>2</sub>O, Xiao et al. (2013))  
515 but similar to the value for WUE<sub>e</sub> based on NEP and ET in mangroves (0.77 g C kg<sup>-1</sup> H<sub>2</sub>O,  
516 Krauss et al. (2022)), which are also C3 plants. The Chinese saltmarshes studied in Xiao et al.  
517 (2013) are dominated by *Spartina alterniflora*, a C4 perennial grass. C4 plants have higher  
518 (often double) water use efficiencies than C3 plants due to CO<sub>2</sub> concentrating mechanisms  
519 (Osborne and Freckleton, 2009). The saltmarsh at French Island includes only C3 plants, and  
520 the dominant chenopod *Sarcocornia quinqueflora* has been suspected to have higher  
521 evapotranspiration rates than saltmarsh by approx. 15% (Hughes et al., 2001), but while

522 *Sarcocornia quinqueflora* dominates at this site, the footprint is a mix of species, and the  
523 lower WUE<sub>e</sub> cannot be directly linked to the presence of *Sarcocornia quinqueflora*.  
524 Furthermore, like most wetlands, the wetland surface is a mixed composition of emergent  
525 vegetation, unsaturated soil and water bodies thus the spatial scale at which WUE<sub>e</sub> is  
526 determined encompasses both the canopy (E<sub>c</sub>) as well as any open water present in the  
527 footprint. Transpiration is predicted to account for only 55% of ET in these systems (Hughes  
528 et al., 2001), which is an E<sub>c</sub> to ET ratio similar to that of mangroves (Krauss et al., 2022) but  
529 significantly lower than terrestrial forests where more than 90% of ET can be attributed to  
530 transpiration. Thus, regional variations in WUE<sub>e</sub> can be attributed to multiple forcings that  
531 form complex spatiotemporal patterns.

532  
533 Saltmarshes are considered among the most productive ecosystems on Earth with an  
534 estimated global NEP of 634 Tg C y<sup>-1</sup> (Fagherazzi et al., 2013) and 601 634 Tg C y<sup>-1</sup>  
535 (Rosentreter et al., 2023). Productivity of southern Australian marshes was previously  
536 estimated at 0.8 kg m<sup>-2</sup> y<sup>-1</sup> by repeated measurements of above ground standing crops (Clarke  
537 and Jacoby, 1994), which if not accounting for season, equates to 2.2 g C m<sup>-2</sup> d<sup>-1</sup>. Similar  
538 studies on saltmarshes in France report lower productivity (483 g C m<sup>-2</sup> y<sup>-1</sup>, (Mayen et al.,  
539 2024)) and daily growing season rates of 1.53 g C m<sup>-2</sup> d<sup>-1</sup>, but mid-latitude saltmarsh sites in  
540 the USA and China show productivity rates of 775 g C m<sup>-2</sup> y<sup>-1</sup>, (Wang et al., 2016) and 668 g  
541 C m<sup>-2</sup> y<sup>-1</sup>, (Xiao et al., 2013) respectively. It is clear that productivity across climate zones  
542 and biogeographic regions varies widely with some studies even reporting net emissions over  
543 an annual period from some marshes and a global average estimated between 382 (Alongi,  
544 2020) and 1,585 g C m<sup>-2</sup> y<sup>-1</sup> (Chmura et al., 2003), albeit based on a small subset of studies.  
545 An analysis of GPP across latitudes in the USA show that warmer sites (including mangrove  
546 wetlands in southern USA) had significantly higher GPP than mid-latitude saltmarshes such  
547 as the one on French Island (Feagin et al., 2020). Mangroves have higher NEE than  
548 saltmarshes, estimated by Krauss et al. (2022) to average 1200 g C m<sup>-2</sup> y<sup>-1</sup>. While our data  
549 does not provide enough coverage for a long-term annual estimate of carbon flux, our daily  
550 values of an average of 2.88 g C m<sup>-2</sup> d<sup>-1</sup> during the growing season, combined with the  
551 relatively short dormant season relative to other temperate locations, suggest a high carbon  
552 sequestration rate for this ecosystem type. In another southern hemisphere study, growing  
553 season rates at an EC tower site in Argentina, are extrapolated by us to average 1.6 g C m<sup>-2</sup> d<sup>-1</sup>  
554 (Bautista et al., 2023) but in that saltmarsh, flooding reduced vegetation biomass and  
555 productivity.

556

557 The data presented here is the exchange of carbon between the land surface and the  
558 atmosphere, but saltmarshes, like other marine connected communities, exchange carbon also  
559 through dissolved carbon pathways, which can be significant (Cai, 2011). Thus, the fluxes  
560 presented here do not constitute the entire carbon budget of this ecosystem.

561

## 562 5 Conclusions

563

564 The response of the French Island saltmarsh to environmental drivers is indicative of the  
565 complex interactions determining saltmarsh productivity. The unique long-term, high-  
566 resolution record enabled us to derive temperature, VPD and light response functions, thus  
567 formulating equations that describe how climate-change sensitive parameters such as  
568 temperature, relative humidity, and cloud cover, affect CO<sub>2</sub> uptake, respiration and  
569 evapotranspiration. The marsh operated as a CO<sub>2</sub> sink throughout the various canopy  
570 phenological phases, but during the dormant period, CO<sub>2</sub> uptake was less than 25% that of  
571 the growing season. Seasonality of greenhouse gas fluxes in Australian saltmarshes is an  
572 understudied but important aspect of global carbon budgeting.

573

## 574 Competing interests

575

576 The contact author has declared that none of the authors has any competing interests.

577

## 578 Acknowledgments

579

580 The work was carried out with the permission of Parks Victoria (Permit 10008684). We thank  
581 Phil and Yuko Bock for logistic support and accommodation on French Island. We thank  
582 Leigh Burgess, Kiri Mason and Ian McHugh for technical support and the Australian OzFlux  
583 community for ongoing collaboration. This work was funded by an Australian Research  
584 Council Discovery Award to RR and ED (DP220102873) as well as a Monash University  
585 Networks of Excellence award to RR.

586

## 587 Data Availability

588 Data used for this analysis is available at <https://figshare.com/s/ba62aafd1a4049248a08> (note  
589 that this is a temporary private link to an embargoed dataset which will be replaced with a  
590 publicly available DOI upon publication).

591

592 Author contribution

593 RR conceptualised the study, acquired funding, prepared the manuscript, designed and  
594 carried out the field campaign, and performed the analysis. ED acquired funding, developed  
595 methodology and prepared the manuscript. AG developed methodology and prepared the  
596 manuscript. TA, EJVH, HR and MP were involved in the field investigation and  
597 administration of the project and provided edits on the manuscript.

598

599 References

600

601 Adam, P.: Saltmarsh Ecology, Cambridge University Press, 1990.

602 Adam, P.: Morecambe Bay saltmarshes: 25 years of change, in: British Saltmarshes, Forrest  
603 Text, Cardigan, UK, 81–107, 2000.

604 Adam, P.: Saltmarshes in a time of change, *Environ. Conserv.*, 29, 39–61,  
605 <https://doi.org/10.1017/S0376892902000048>, 2002.

606 Alongi, D. M.: Carbon balance in salt marsh and mangrove ecosystems: A global synthesis, *J.*  
607 *Mar. Sci. Eng.*, 8, 767, 2020.

608 Artigas, F., Shin, J. Y., Hobbie, C., Marti-Donati, A., Schäfer, K. V. R., and Pechmann, I.:  
609 Long term carbon storage potential and CO<sub>2</sub> sink strength of a restored salt marsh in New  
610 Jersey, *Agric. For. Meteorol.*, 200, 313–321, <https://doi.org/10.1016/j.agrformet.2014.09.012>,  
611 2015.

612 Baldocchi, D. D.: Assessing the eddy covariance technique for evaluating carbon dioxide  
613 exchange rates of ecosystems: past, present and future, *Glob. Change Biol.*, 9, 479–492,  
614 <https://doi.org/10.1046/j.1365-2486.2003.00629.x>, 2003.

615 Barr, A. G., Richardson, A. D., Hollinger, D. Y., Papale, D., Arain, M. A., Black, T. A.,  
616 Bohrer, G., Dragoni, D., Fischer, M. L., Gu, L., Law, B. E., Margolis, H. A., McCaughey, J.  
617 H., Munger, J. W., Oechel, W., and Schaeffer, K.: Use of change-point detection for friction-  
618 velocity threshold evaluation in eddy-covariance studies, *Agric. For. Meteorol.*, 171, 31–45,  
619 <https://doi.org/10.1016/j.agrformet.2012.11.023>, 2013.

620

621 Bautista, N. E., Gassmann, M. I. , and Pérez, C. F.: Gross primary production, ecosystem  
622 respiration, and net ecosystem production in a southeastern South American salt marsh.  
623 *Estuaries Coast*, 46, 1923–1937, <https://doi.org/10.1007/s12237-023-01224-8>, 2023.

624



- 625 Berry, J., and Björkman, O.: Photosynthetic response and adaptation to temperature in higher  
626 plants, *Ann. Rev. Plant Physiol.*, 31, 491-543,  
627 <https://doi.org/10.1146/annurev.pp.31.060180.002423>, 1980.  
628
- 629 Borges, A. V., Schiettecatte, L.-S., Abril, G., Delille, B., and Gazeau, F.: Carbon dioxide in  
630 European coastal waters, *Trace Gases Eur. Coast. Zone*, 70, 375–387,  
631 <https://doi.org/10.1016/j.ecss.2006.05.046>, 2006.
- 632 Cai, W.-J.: Estuarine and coastal ocean carbon paradox: CO<sub>2</sub> sinks or sites of terrestrial  
633 carbon incineration?, *Annu. Rev. Mar. Sci.*, 3, 123–145, [https://doi.org/10.1146/annurev-](https://doi.org/10.1146/annurev-marine-120709-142723)  
634 [marine-120709-142723](https://doi.org/10.1146/annurev-marine-120709-142723), 2011.
- 635 Chen, J., Falk, M., Euskirchen, E., Paw U, K. T., Suchanek, T. H., Ustin, S. L., Bond, B. J.,  
636 Brosofske, K. D., Phillips, N., and Bi, R.: Biophysical controls of carbon flows in three  
637 successional Douglas-fir stands based on eddy-covariance measurements, *Tree Physiol.*, 22,  
638 169–177, <https://doi.org/10.1093/treephys/22.2-3.169>, 2002.
- 639 Chmura, G. L., Anisfeld, S. C., Cahoon, D. R., and Lynch, J. C.: Global carbon sequestration  
640 in tidal, saline wetland soils, *Glob. Biogeochem. Cycles*, 17,  
641 <https://doi.org/10.1029/2002GB001917>, 2003.
- 642 Clarke, P., J. and Jacoby, C. A.: Biomass and above-ground productivity of salt-marsh plants  
643 in South-eastern Australia, *Aust. J. Mar. Freshw. Res.*, 45, 1521–1528, 1994.
- 644 Davis, K. J., Bakwin, P. S., Yi, C., Berger, B. W., Zhao, C., Teclaw, R. M., and Isebrands, J.  
645 G.: The annual cycles of CO<sub>2</sub> and H<sub>2</sub>O exchange over a northern mixed forest as observed  
646 from a very tall tower, *Glob. Change Biol.*, 9, 1241-1332, [https://doi.org/10.1046/j.1365-](https://doi.org/10.1046/j.1365-2486.2003.00672.x)  
647 [2486.2003.00672.x](https://doi.org/10.1046/j.1365-2486.2003.00672.x), 2003.
- 648 Drake, B. G.: Photosynthesis of salt marsh species, *Aquat. Bot.*, 34, 167-180,  
649 [https://doi.org/10.1016/0304-3770\(89\)90055-7](https://doi.org/10.1016/0304-3770(89)90055-7), 1989.  
650
- 651 Duarte, C. M.: Reviews and syntheses: Hidden forests, the role of vegetated coastal habitats  
652 in the ocean carbon budget, *Biogeosciences*, 14, 301–310, [https://doi.org/10.5194/bg-14-301-](https://doi.org/10.5194/bg-14-301-2017)  
653 [2017](https://doi.org/10.5194/bg-14-301-2017), 2017.
- 654 Erickson, J. E., Peresta, G., Montovan, K. J., and Drake, B. G.: Direct and indirect effects of  
655 elevated atmospheric CO<sub>2</sub> on net ecosystem production in a Chesapeake Bay tidal wetland,  
656 *Glob. Change Biol.*, 19, 3368–3378, 2013.
- 657 Fagherazzi, S., Wiberg, P. L., Temmerman, S., Struyf, E., Zhao, Y., and Raymond, P. A.:  
658 Fluxes of water, sediments, and biogeochemical compounds in salt marshes, *Ecol. Process.*,  
659 2, 3, <https://doi.org/10.1186/2192-1709-2-3>, 2013.
- 660 Feagin, R. A., Forbrich, I., Huff, T. P., Barr, J. G., Ruiz-Plancarte, J., Fuentes, J. D., Najjar,  
661 R. G., Vargas, R., Vázquez-Lule, A., Windham-Myers, L., Kroeger, K. D., Ward, E. J.,  
662 Moore, G. W., Leclerc, M., Krauss, K. W., Stagg, C. L., Alber, M., Knox, S. H., Schäfer, K.  
663 V. R., Bianchi, T. S., Hutchings, J. A., Nahrawi, H., Noormets, A., Mitra, B., Jaimes, A.,  
664 Hinson, A. L., Bergamaschi, B., King, J. S., and Miao, G.: Tidal wetland gross primary  
665 production across the continental United States, 2000–2019, *Glob. Biogeochem. Cycles*, 34,  
666 [e2019GB006349](https://doi.org/10.1029/2019GB006349), <https://doi.org/10.1029/2019GB006349>, 2020.

667 Feher, L. C., Osland, M. J., Griffith, K. T., Grace, J. B., Howard, R. J., Stagg, C. L.,  
668 Enwright, N. M., Krauss, K. W., Gabler, C. A., Day, R. H., and Rogers, K.: Linear and  
669 nonlinear effects of temperature and precipitation on ecosystem properties in tidal saline  
670 wetlands, *Ecosphere*, 8, e01956, <https://doi.org/10.1002/ecs2.1956>, 2017.

671 Gedan, K. B., Silliman, B. R., and Bertness, M. D.: Centuries of human-driven change in salt  
672 marsh ecosystems, *Annu. Rev. Mar. Sci.*, 1, 117–141,  
673 <https://doi.org/10.1146/annurev.marine.010908.163930>, 2009.

674 Ghosh, S. and Mishra, D. R.: Analyzing the long-term phenological trends of salt marsh  
675 ecosystem across coastal Louisiana, *Remote Sens.*, 9, <https://doi.org/10.3390/rs9121340>,  
676 2017.

677 Giurgevich, J. R. and Dunn, E. L.: A comparative analysis of the CO<sub>2</sub> and water vapor  
678 responses of two *Spartina* species from Georgia coastal marshes, *Estuar. Coast. Shelf Sci.*,  
679 12, 561–568, [https://doi.org/10.1016/S0302-3524\(81\)80082-5](https://doi.org/10.1016/S0302-3524(81)80082-5), 1981.

680 Hilker, T., Hall, F. G., Coops, N. C., Lyapustin, A., Wang, Y., Nesic, Z., Grant, N., Black, T.  
681 A., Wulder, M. A., Kljun, N., Hopkinson, C., and Chasmer, L.: Remote sensing of  
682 photosynthetic light-use efficiency across two forested biomes: Spatial scaling, *Remote Sens.*  
683 *Environ.*, 114, 2863–2874, <https://doi.org/10.1016/j.rse.2010.07.004>, 2010.

684 Hill, A. C. and Vargas, R.: Methane and carbon dioxide fluxes in a temperate tidal salt marsh:  
685 comparisons between plot and ecosystem measurements, *J. Geophys. Res. Biogeosciences*,  
686 127, e2022JG006943, <https://doi.org/10.1029/2022JG006943>, 2022.

687 Howe, A. J., Rodríguez, J. F., Spencer, J., MacFarlane, G. R., and Saintilan, N.: Response of  
688 estuarine wetlands to reinstatement of tidal flows, *Mar. Freshw. Res.*, 61, 702–713, 2010.

689 Hughes, C. E., Kalma, J. D., Binning, P., Willgoose, G. R., and Vertzonis, M.: Estimating  
690 evapotranspiration for a temperate salt marsh, Newcastle, Australia, *Hydrol. Process.*, 15,  
691 957–975, <https://doi.org/10.1002/hyp.189>, 2001.

692 Huxham, M., Whitlock, D., Githaiga, M., and Dencer-Brown, A.: Carbon in the coastal  
693 seascape: how interactions between mangrove forests, seagrass meadows and tidal marshes  
694 influence carbon storage, *Curr. For. Rep.*, 4, 101–110, <https://doi.org/10.1007/s40725-018-0077-4>, 2018.

696 Kathilankal, J. C., Mozdzer, T. J., Fuentes, J. D., D’Odorico, P., McGlathery, K. J., and  
697 Zieman, J. C.: Tidal influences on carbon assimilation by a salt marsh, *Environ. Res. Lett.*, 3,  
698 044010, <https://doi.org/10.1088/1748-9326/3/4/044010>, 2008.

699 Kljun, N., Calanca, P., Rotach, M. W., and Schmid, H. P.: A simple two-dimensional  
700 parameterisation for Flux Footprint Prediction (FFP), *Geosci Model Dev*, 8, 3695–3713,  
701 <https://doi.org/10.5194/gmd-8-3695-2015>, 2015.

702 Krauss, K. W., Lovelock, C. E., Chen, L., Berger, U., Ball, M. C., Reef, R., Peters, R.,  
703 Bowen, H., Vovides, A. G., Ward, E. J., and others: Mangroves provide blue carbon  
704 ecological value at a low freshwater cost, *Sci. Rep.*, 12, <https://doi.org/10.1038/s41598-022-13000-0>, 2022.

705 Lloyd, J., and Taylor, J. A.: On the temperature dependence of soil respiration, *Funct. Ecol.*,  
706 8(3), 315–323. <https://doi.org/10.2307/2389824>, 1994.

707  
708 Lu, W., Xiao, J., Liu, F., Zhang, Y., Liu, C., and Lin, G.: Contrasting ecosystem CO<sub>2</sub> fluxes  
709 of inland and coastal wetlands: a meta-analysis of eddy covariance data, *Glob. Change Biol.*,  
710 23, 1180–1198, <https://doi.org/10.1111/gcb.13424>, 2017.

711 Mayen, J., Polsenaere, P., Lamaud, É., Arnaud, M., Kostyrka, P., Bonnefond, J.-M., Geairon,  
712 P., Gernigon, J., Chassagne, R., and Lacoue-Labarthe, T.: Atmospheric CO<sub>2</sub> exchanges  
713 measured by eddy covariance over a temperate salt marsh and influence of environmental  
714 controlling factors, *Biogeosciences*, 21, 993–1016, 2024.

715 McLeod, E., Chmura, G. L., Bouillon, S., Salm, R., Björk, M., Duarte, C. M., Lovelock, C.  
716 E., Schlesinger, W. H., and Silliman, B. R.: A blueprint for blue carbon: toward an improved  
717 understanding of the role of vegetated coastal habitats in sequestering CO<sub>2</sub>, *Front. Ecol.*  
718 *Environ.*, 9, 552–560, <https://doi.org/10.1890/110004>, 2011.

719 Mcowen, C. J., Weatherdon, L. V., Bochove, J.-W. V., Sullivan, E., Blyth, S., Zockler, C.,  
720 Stanwell-Smith, D., Kingston, N., Martin, C. S., Spalding, M., and Fletcher, S.: A global map  
721 of saltmarshes, *Biodivers. Data J.*, 5, e11764, <https://doi.org/10.3897/BDJ.5.e11764>, 2017.

722 McVicar, T., Vleeshouwer, J., Van Niel, T., Guerschman, J., and Peña-Arancibia, J. L.:  
723 Actual Evapotranspiration for Australia using CMRSET algorithm. Version 1.0, 2022.

724 Mitsch, W. J. and Gosselink, J. G.: The value of wetlands: importance of scale and landscape  
725 setting, *Ecol. Econ.*, 35, 25–33, [https://doi.org/10.1016/S0921-8009\(00\)00165-8](https://doi.org/10.1016/S0921-8009(00)00165-8), 2000.

726 Moffett, K. B., Wolf, A., Berry, J. A., and Gorelick, S. M.: Salt marsh–atmosphere exchange  
727 of energy, water vapor, and carbon dioxide: Effects of tidal flooding and biophysical controls,  
728 *Water Resour. Res.*, 46, 2010.

729 Nahrawi, H., Leclerc, M. Y., Pennings, S., Zhang, G., Singh, N., and Pahari, R.: Impact of  
730 tidal inundation on the net ecosystem exchange in daytime conditions in a salt marsh, *Agric.*  
731 *For. Meteorol.*, 294, 108133, <https://doi.org/10.1016/j.agrformet.2020.108133>, 2020.

732 Navarro, A., Young, M., Macreadie, P. I., Nicholson, E., and Ierodiaconou, D.: Mangrove  
733 and saltmarsh distribution mapping and land cover change assessment for south-eastern  
734 Australia from 1991 to 2015, *Remote Sens.*, 13, <https://doi.org/10.3390/rs13081450>, 2021.

735 Osborne, C. P. and Freckleton, R. P.: Ecological selection pressures for C<sub>4</sub> photosynthesis in  
736 the grasses. *Proc. Roc. Soc. B*, 276, <https://doi.org/10.1098/rspb.2008.1762>, 2009.

737 Otani, S. and Endo, T.: CO<sub>2</sub> flux in tidal flats and salt marshes, *Blue Carbon Shallow Coast.*  
738 *Ecosyst. Carbon Dyn. Policy Implement.*, 223–250, 2019.

739 Owers, C. J., Rogers, K. and Woodroffe, C. D.: Spatial variation of above-ground carbon  
740 storage in temperate coastal wetlands. *Estuar. Coast. Shelf Sci.*, 210, 55–67,  
741 <https://doi.org/10.1016/j.ecss.2018.06.002>, 2018  
742

743 R Core Team: R: A Language Environment for Statistical Computing. Vienna, Australia,  
744 2024.

745 Reents, S., Möller, I., Evans, B. R., Schoutens, K., Jensen, K., Paul, M., Bouma, T. J.,  
746 Temmerman, S., Lustig, J., Kudella, M., and Nolte, S.: Species-specific and seasonal

- 747 differences in the resistance of salt-marsh vegetation to wave impact, *Front. Mar. Sci.*, 9,  
748 2022.
- 749 Rosentreter, J. A., Laruelle, G. G., Bange, H. W., Bianchi, T. S., Busecke, J. J. M., Cai, W. J.,  
750 Eyre, B. D., Forbich, I., Kwon, E. Y., Maavara, T., Moosdorf, N., Najjar, R. G., Sarma, V. V.  
751 S. S., Van Dam, B. and Regnier, P.: Coastal vegetation and estuaries are collectively a  
752 greenhouse gas sink. *Nat. Clim. Chang.* 13, 579–587. [https://doi.org/10.1038/s41558-023-](https://doi.org/10.1038/s41558-023-01682-9)  
753 [01682-9](https://doi.org/10.1038/s41558-023-01682-9), 2023.
- 754  
755 Schäfer, K. V. R., Duman, T., Tomasicchio, K., Tripathee, R., and Sturtevant, C.: Carbon  
756 dioxide fluxes of temperate urban wetlands with different restoration history, *Agric. For.*  
757 *Meteorol.*, 275, 223–232, <https://doi.org/10.1016/j.agrformet.2019.05.026>, 2019.
- 758 Seyfferth, A. L., Bothfeld, F., Vargas, R., Stuckey, J. W., Wang, J., Kearns, K., Michael, H.  
759 A., Guimond, J., Yu, X., and Sparks, D. L.: Spatial and temporal heterogeneity of  
760 geochemical controls on carbon cycling in a tidal salt marsh, *Geochim. Cosmochim. Acta*,  
761 282, 1–18, 2020.
- 762 Shepard, C. C., Crain, C. M., and Beck, M. W.: The protective role of coastal marshes: a  
763 systematic review and meta-analysis, *PLoS ONE*, 6, e27374,  
764 <https://doi.org/10.1371/journal.pone.0027374>, 2011.
- 765 Smith, J. A. M., Regan, K., Cooper, N. W., Johnson, L., Olson, E., Green, A., Tash, J., Evers,  
766 D. C., and Marra, P. P.: A green wave of saltmarsh productivity predicts the timing of the  
767 annual cycle in a long-distance migratory shorebird, *Sci. Rep.*, 10, 20658,  
768 <https://doi.org/10.1038/s41598-020-77784-7>, 2020.
- 769 Vázquez-Lule, A. and Vargas, R.: Biophysical drivers of net ecosystem and methane  
770 exchange across phenological phases in a tidal salt marsh, *Agric. For. Meteorol.*, 300,  
771 108309, <https://doi.org/10.1016/j.agrformet.2020.108309>, 2021.
- 772 Wang, Z. A., Kroeger, K. D., Ganju, N. K., Gonnee, M. E., and Chu, S. N.: Intertidal salt  
773 marshes as an important source of inorganic carbon to the coastal ocean, *Limnol. Oceanogr.*,  
774 61, 1916–1931, <https://doi.org/10.1002/lno.10347>, 2016.
- 775 Ward, N. D., Megonigal, J. P., Bond-Lamberty, B., Bailey, V. L., Butman, D., Canuel, E. A.,  
776 Diefenderfer, H., Ganju, N. K., Goñi, M. A., and Graham, E. B.: Representing the function  
777 and sensitivity of coastal interfaces in Earth system models, *Nat. Commun.*, 11, 2458, 2020.
- 778 Wei, S., Han, G., Jia, X., Song, W., Chu, X., He, W., Xia, J., and Wu, H.: Tidal effects on  
779 ecosystem CO<sub>2</sub> exchange at multiple timescales in a salt marsh in the Yellow River Delta,  
780 *Estuar. Coast. Shelf Sci.*, 238, 106727, 2020.
- 781 Whitfield, A. K.: The role of seagrass meadows, mangrove forests, salt marshes and reed  
782 beds as nursery areas and food sources for fishes in estuaries, *Rev. Fish Biol. Fish.*, 27, 75–  
783 110, <https://doi.org/10.1007/s11160-016-9454-x>, 2017.
- 784 Xiao, J., Sun, G., Chen, J., Chen, H., Chen, S., Dong, G., Gao, S., Guo, H., Guo, J., Han, S.,  
785 Kato, T., Li, Y., Lin, G., Lu, W., Ma, M., McNulty, S., Shao, C., Wang, X., Xie, X., Zhang,  
786 X., Zhang, Z., Zhao, B., Zhou, G., and Zhou, J.: Carbon fluxes, evapotranspiration, and water

787 use efficiency of terrestrial ecosystems in China, *Agric. For. Meteorol.*, 182–183, 76–90,  
788 <https://doi.org/10.1016/j.agrformet.2013.08.007>, 2013.

789